Journal of Power Sources 195 (2010) 6373–6378

Contents lists available at ScienceDirect

Journal of Power Sources

journal homepage: www.elsevier.com/locate/jpowsour

Activity and stability of non-precious metal catalysts for oxygen reduction in acid and alkaline electrolytes

Xuguang Li, Gang Liu, Branko N. Popov*

Center for Electrochemical Engineering, Department of Chemical Engineering, University of South Carolina, Columbia, SC 29208, USA

ARTICLE INFO

Article history:
Received 8 March 2010
Received in revised form 6 April 2010
Accepted 7 April 2010
Available online 13 April 2010

Keywords:
Non-precious metal catalyst
Stability
Activity
Oxygen reduction reaction
Alkaline electrolyte
Fuel cell

ABSTRACT

The activity and stability of non-precious metal catalysts (NPMCs) for the oxygen reduction reaction (ORR) in both acid and alkaline electrolytes were studied by the rotating disk electrode technique. The NPMCs were prepared through the pyrolysis of cobalt–iron–nitrogen chelate followed by combination of pyrolysis, acid leaching, and re-pyrolysis. In both environments, the catalysts heat-treated at 800–900 °C exhibited relatively high activity. Particularly, an onset potential of 0.92 V and a well-defined limiting current plateau for the ORR was observed in alkaline medium. The potential cycling stability test revealed the poor stability of NPMCs in acid solution with an exponential increase in the performance degradation as a function of the number of potential cycling. In contrast, the NPMCs demonstrated exceptional stability in alkaline solution. The numbers of electron transferred during the ORR on the NPMCs in acid and alkaline electrolytes were 3.65 and 3.92, respectively, and these numbers did not change before and after the stability test. XPS analysis indicated that the N-containing sites of catalysts are stable before and after the stability test when in alkaline solution but not in acid solution.

1. Introduction

In the past four decades, non-precious metal catalysts (NPMCs) have been extensively studied as a low-cost catalyst alternative to Pt for the oxygen reduction reaction (ORR) in polymer electrolyte membrane (PEM) fuel cells. Though Jasinski discovered the electrocatalytic activity of Co phthalocyanines for the ORR in alkaline media [1], the subsequent studies on the NPMCs as oxygen reduction catalysts have mainly focused on acid electrolytes. Many efforts have been made to improve the activity and stability of the catalysts as well as to clarify the nature of the active sites of NPMCs for the ORR in acid medium. A heat-treatment at high temperatures under an inert atmosphere was found to be able to improve both the activity and stability of carbon-supported metal chelates for oxygen reduction [2,3]. In 1989, Gupta et al. [4] reported that NPMCs can be prepared by pyrolyzing a mixture of polyacrylonitrile and cobalt and iron salts instead of the conventional transition metal macrocycles. Very recently, Lefevre et al. [5] prepared highly active catalysts when a mixture of carbon support, phenanthroline, and ferrous acetate was ball-milled and pyrolized in argon and then ammonia. The best NPMC developed so far has a high initial activity with turnover frequencies matching those of Pt/C; however, its stability is still unsatisfactory. The following consensuses have been reached on the NPMCs [2–5]: (i) the simultaneous presence of transition metal, carbon, and nitrogen play important role in formation of active sites of the catalysts; (ii) the nitrogen is crucial component of the active sites; (iii) the catalysts prepared with Co- and/or Fe-containing precursors is more active compared to other transition metal (non-precious metal) precursors.

Poor stability in acid electrolytes is a major problem of non-precious metal catalysts [5–35]. This is generally attributed to the oxidative corrosion of the carbon support and active sites of the catalysts caused by the hydrogen peroxide (H_2O_2) that is formed during the two-electron reduction of oxygen [15,16]. Recently, a protonation reaction model was proposed by our group to explain the poor stability of the NPMCs in acid electrolytes [28–30]. In the past six years, we have systematically studied the activity and the nature of the active sites of NPMCs for the ORR [26–33]. The highly active NPMCs have been prepared by subjecting carbon-supported nitrogen-metal chelates or nitrogen-containing organic compound-modified carbon black to a treatment combination of pyrolysis, leaching, and re-pyrolysis. According to physical, chemical, and electrochemical investigation [27–30] as well as the literature [36–40], the pyridinic-N and graphitic-N are believed to play important roles in the active sites of NPMCs. The pyridinic-N is a type of nitrogen that bonds to two carbon atoms in the carbon plane with a basic lone pair of electrons. Since the lone pair of electrons is not delocalized into the aromatic π-system, the pyridinic-N

* Corresponding author at: Department of Chemical Engineering, University of South Carolina, Swearingen Engineering Building, 301 Main Street, Columbia, SC 29208, USA. Tel.: +1 803 777 7314; fax: +1 803 777 8265.
E-mail address: popov@cec.sc.edu (B.N. Popov).

0378-7753/$ – see front matter © 2010 Elsevier B.V. All rights reserved.
doi:10.1016/j.jpowsour.2010.04.019

can be protonated to form a pyridinic-N–H (a pyridinium) in the acid electrolyte, which was demonstrated by XPS analysis of the catalysts before and after the fuel cell stability test. The transition of pyridinic-N to pyridinic-N–H may be at least partially responsible for the fast performance degradation of NPMC-based fuel cells [28–30].

In order to further clarify the nature of the active sites of NPMCs, the electrocatalytic properties of the NPMCs for oxygen reduction in alkaline electrolyte was investigated by the rotating disk electrode (RDE) technique. For comparison, the performance of the NPMCs in acid electrolyte was also measured. Specifically, the potential cycling method was employed to evaluate the stability of NPMCs. XPS analysis was conducted to examine the N species before and after the stability test in acid and alkaline electrolytes.

2. Experimental

2.1. Synthesis of the catalysts

The non-precious metal catalysts (NPMCs) were synthesized according to a revised procedure [28]. Briefly, ethylene diamine ($NH_2CH_2CH_2NH_2$) was added to a $Co(NO_3)_2$ and $FeSO_4$ solution, followed by the addition of carbon black. The reaction mixture was refluxed at 85 °C for 4 h and then dried using a rotary evaporator at 80 °C under reduced pressure. The dried sample was heated to 800–1100 °C under an argon atmosphere for 10 h. The heat-treated sample was leached in 0.5 M H_2SO_4 at 80 °C to remove excess metals on the surface of the catalyst. The resulting samples were filtered, washed, and then heat-treated again at 800–1100 °C under an argon atmosphere for 10 h. For convenience, the catalysts heat-treated at different temperatures were denoted as NPMC-800, -900, -950, -1000, and -1100, respectively.

2.2. RDE measurements

RDE measurements were performed in a standard three-compartment electrochemical cell. A glassy carbon disk (5.61 mm diameter) was used as the working electrode. Mercury/mercurous sulfate electrode (Hg/Hg_2SO_4) and mercury/mercury oxide (Hg/HgO) were used as the reference electrode in acid and alkaline electrolyte, respectively, while platinum foil was used as the counter electrode. A 0.5 M H_2SO_4 solution and 0.1 M KOH were used as the electrolytes. All potentials in this work are referenced to a reversible hydrogen electrode (RHE). The catalyst ink was prepared by mixing 8 mg of the catalyst with 1 mL of isopropyl alcohol. Then 15 μL of the ink was deposited onto the glassy carbon. After the deposition, 5 μL of a 0.25 wt.% Nafion solution was applied onto the catalyst layer. The electrode was scanned in N_2-saturated electrolyte at a sweep rate of 5 mV s^{-1} to evaluate the background capacitance current. Linear sweep voltammograms in O_2-saturated electrolyte were measured at 900 rpm. The oxygen reduction current was determined as the difference between currents measured in the nitrogen- and oxygen-saturated electrolytes.

The potential cycling test was performed between 0.8 and 1.2 V in N_2-saturated electrolytes with a potential scan rate of 10 mV s^{-1}. To the best of our knowledge, there is no a standard test protocol to evaluate the stability of the NPMCs. The information on the methods to measure the stability of the NPMCs is relatively scarce. The potential range of 0.8–1.2 V for the potential cycling stability test in this study was based on: (i) catalyst and support accelerated stress test protocols for PEM fuel cells suggested by DOE [41]. In this protocol, the electrode is hold at 1.2 V to examine the stability of the support. The cycling in the potential range of 0.7–0.9 V is used to evaluate the stability of catalyst. (ii) Choo et al. [42] reported that the cycling in the potential range of 0.8–1.0 V can effectively corrode the graphite. Moreover, the corrosion reaction of carbon materials is accelerated by potential cycling compared with potential holding at a certain potential.

2.3. XPS

XPS measurements were carried out on a Kratos AXIS Ultra DLD XPS system equipped with a hemispherical energy analyzer and a monochromatic Al Kα source, which was operated at 15 keV and 150 W.

3. Results and discussion

Fig. 1a shows the polarization curves for the oxygen reduction reaction in O_2-saturated 0.5 M H_2SO_4 on the non-precious metal catalysts (NPMCs) heat-treated at different temperatures. The measurements were conducted using a potential scan rate of 5 mV s^{-1} and an electrode rotation rate of 900 rpm. The catalysts heat-treated at 800 and 900 °C exhibit higher catalytic activity toward the ORR with onset potentials both around 0.88 V. With the further increase of heat-treatment temperatures, the performance of the catalysts gradually decreases. Specifically, the onset potential shows a negative shift from 0.88 to 0.78 V for the catalysts from NPMC-800 to NPMC-1100. At the current density of 1.6 mA cm^{-2}, the potential decreases from 0.73 to 0.71, 0.66, 0.6, and 0.52 V for the catalysts heat-treated at the temperatures ranging from 800 to 1100 °C. This trend is in good agreement with the results previously reported in the literature [7–9,16]. The lower activity of the catalysts heat-treated at higher temperatures may be at least partially attributed to the decreased nitrogen contents while increasing heat-treatment temperatures demonstrated by the XPS analysis. The nitrogen surface contents (at.%) decreases in the order: NPMC-800 (2.11) > NPMC-900 (2.06) > NPMC-950 (1.18) > NPMC-1000 (0.77) > NPMC-1100 (0.40). This is consistent with the activity trend observed in Fig. 1a.

Fig. 1b shows the Tafel plots for the oxygen reduction reaction in O_2-saturated 0.5 M H_2SO_4 on NPMCs heat-treated at different temperatures deduced from Fig. 1a. The polarization curves in Fig. 1a were corrected for diffusion effects using the equation:

$$i_{kin} = \frac{i_l i}{i_l - i} \quad (1)$$

where i_{kin} is the kinetic current density, i_l is the limiting current density, and i is the measured current density. As shown in Fig. 1b, the Tafel slope is about 58 mV dec^{-1} at low current density. This value may be ascribed to the transfer of the first electron as a rate-determining step and the Temkin conditions of intermediate adsorption [43]. The activity difference of the catalysts as a function of heat-treatment temperatures can be clearly identified from the Tafel plot in the low current density region.

Fig. 2a shows the polarization curves for the oxygen reduction reaction on the non-precious metal catalyst heat-treated at 900 °C (NPMC-900) before and after the potential cycling stability test in acid solution. The NPMC-900 was selected since it may be a representative catalyst with both good activity and stability [28–30,32]. The potential cycling test was carried out between 0.8 and 1.2 V in N_2-saturated 0.5 M H_2SO_4 with a potential scan rate of 10 mV s^{-1}. The polarization curves were measured before and after 100, 200, and 700 cycles in O_2-saturated 0.5 M H_2SO_4 using a potential scan rate of 5 mV s^{-1} and an electrode rotation rate of 900 rpm. From Fig. 2a, great performance decay is observed after the first 100 cycles of potential cycling. During the subsequent 600 potential cycles, the extent of activity degradation of catalysts is much smaller. This result is consistent with those reported for the long-term fuel cell/RDE stability test [5–35]. Generally, there are

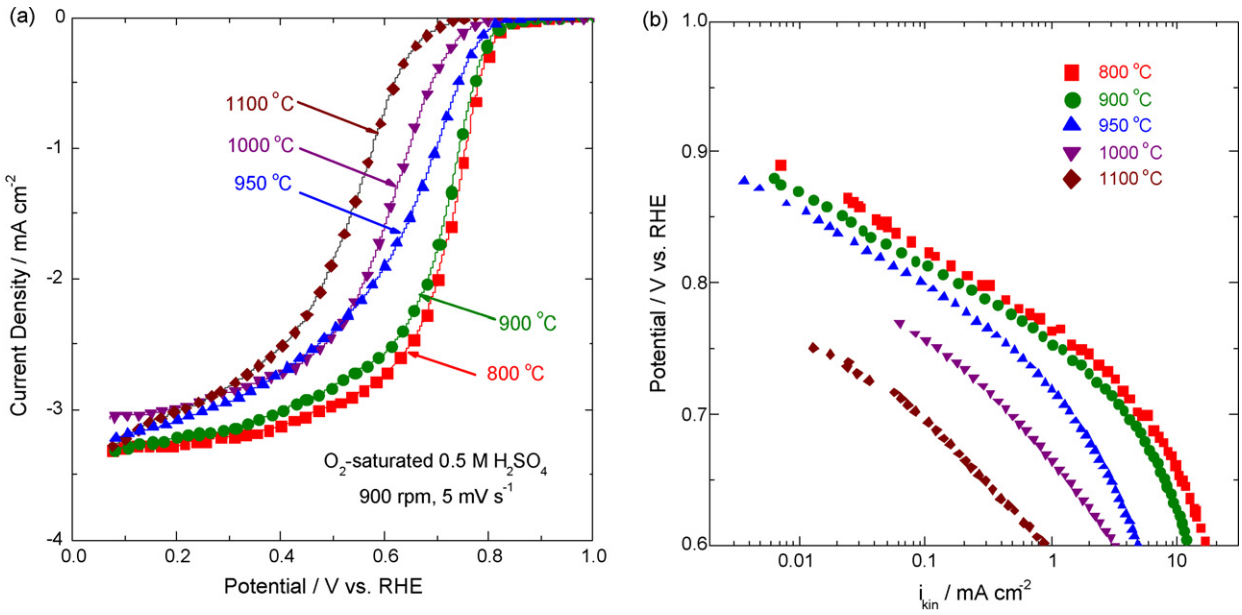

Fig. 1. (a) Polarization curves for the oxygen reduction reaction in O_2-saturated 0.5 M H_2SO_4 on non-precious metal catalysts heat-treated at different temperatures; scan rate: 5 mV s^{-1}; rotation rate: 900 rpm. (b) Tafel plots for the oxygen reduction reaction in O_2-saturated 0.5 M H_2SO_4 on non-precious metal catalysts heat-treated at different temperatures deduced from the polarization curves in a.

two distinct performance degradation stages for an NPMC with an initial higher decay rate and a subsequent lower one. Therefore, the potential cycling method may be a promising protocol to quickly evaluate the stability of the non-precious metal catalysts.

In order to clearly evaluate the stability properties of heat-treated NPMCs, the percentage of potential loss E_{loss}% at 1.6 mA cm^{-2} was calculated and is summarized in Fig. 2b. The E_{loss}% is expressed as follows:

$$E_{loss}\% = \frac{E_{ini} - E}{E_{ini}} \times 100\% \quad (2)$$

where E_{ini} is the initial potential of oxygen reduction on the catalysts at 1.6 mA cm^{-2} and E is the potential after a certain number of potential cycling. It can be seen from Fig. 2b that the percentage of potential loss, E_{loss}%, of the ORR on the NPMCs increases exponentially with increasing numbers of potential cycling. This may indicate some intrinsic relationship between the active sites in NPMCs and the kinetics of the ORR; however, further experimental and modeling research are needed to clarify this relationship. On the other hand, the relative extent of performance degradation on the catalysts heat-treated at lower temperatures is smaller compared to those heat-treated at higher temperatures. This may be at least partially due to the higher initial activity of NPMCs heat-treated at lower temperatures.

Fig. 3a shows the polarization curves for the oxygen reduction reaction in O_2-saturated 0.1 M KOH on NPMCs heat-treated at dif-

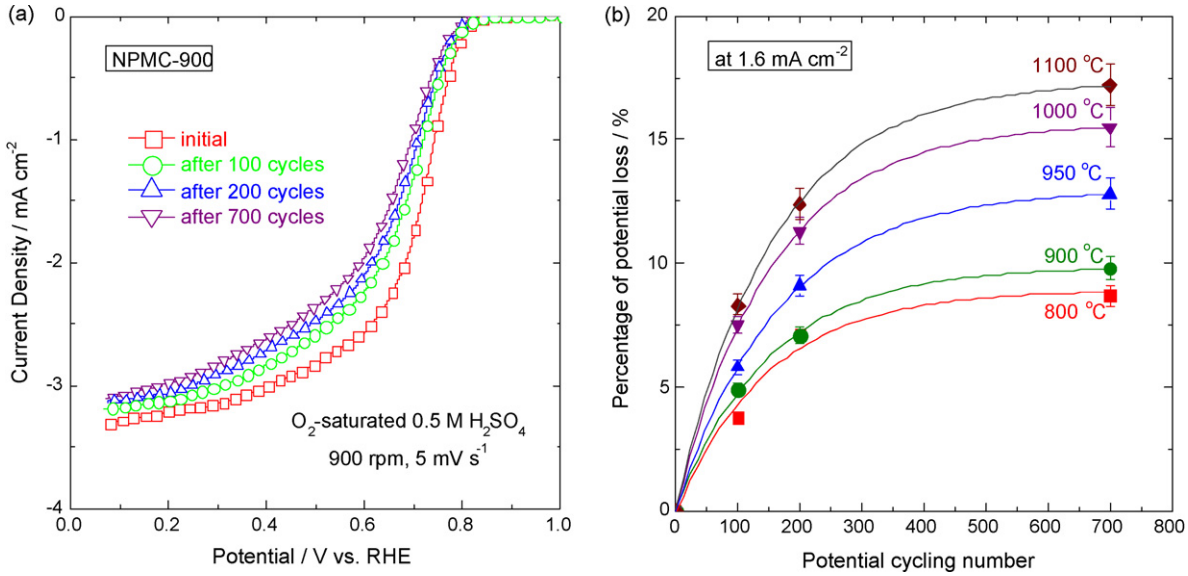

Fig. 2. (a) Polarization curves for the oxygen reduction reaction in O_2-saturated 0.5 M H_2SO_4 on non-precious metal catalysts heat-treated at 900 °C before and after the potential cycling stability test; scan rate: 5 mV s^{-1}; rotation rate: 900 rpm. The potential cycling was performed in N_2-saturated 0.5 M H_2SO_4 with a scan rate of 10 mV s^{-1} between 0.8 and 1.2 V vs. RHE for 100, 200, and 700 cycles. (b) Percentage of potential loss, E_{loss}%, at 1.6 mA cm^{-2} for the oxygen reduction reaction in O_2-saturated 0.5 M H_2SO_4 on non-precious metal catalysts heat-treated at different temperatures as a function of the number of potential cycling.

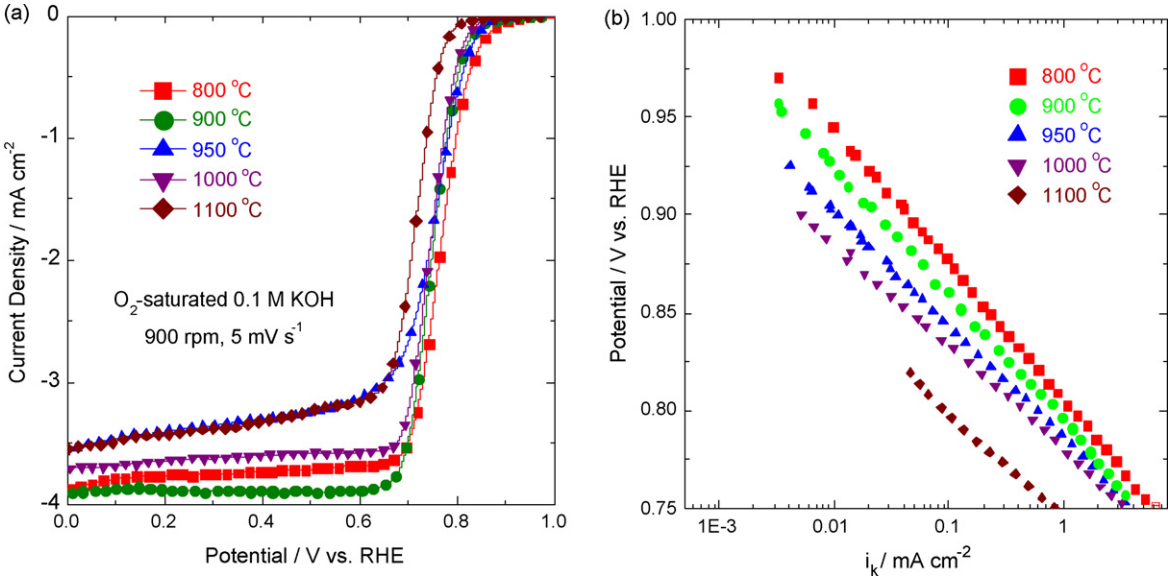

Fig. 3. (a) Polarization curves for the oxygen reduction reaction in O_2-saturated 0.1 M KOH on non-precious metal catalysts heat-treated at different temperatures; scan rate: 5 mV s^{-1}; rotation rate: 900 rpm. (b) Tafel plots for the oxygen reduction reaction in O_2-saturated 0.1 M KOH on non-precious metal catalysts heat-treated at different temperatures deduced from the polarization curves in a.

ferent temperatures. The measurements were conducted using a potential scan rate of 5 mV s^{-1} and an electrode rotation rate of 900 rpm. It is evident that the NPMCs exhibit high activity for the ORR with onset potentials as high as 0.92 V and well-defined limiting current plateaus. The catalysts heat-treated at 800–1000 °C show a relatively higher catalytic performance toward the oxygen reduction, while the performance of NPMC-1100 is lower. Fig. 3b shows the Tafel plots for the ORR in alkaline solution deduced from Fig. 3a with the correction for diffusion effects. The Tafel slopes are in the range of 50–65 mV dec^{-1} for the catalysts from NPMC-1100 to NPMC-800. It is clear that the kinetic current density at a constant potential decreases from the NPMC-800 to NPMC-1100.

Fig. 4 shows the polarization curves for the oxygen reduction reaction on the NPMC-900 before and after the potential cycling test in 0.1 M KOH. The potential cycling test was carried out between 0.8 and 1.2 V in N_2-saturated 0.1 M KOH with a scan rate of 10 mV s^{-1}. The polarization curves were measured before and after 100, 200, and 700 cycles in O_2-saturated 0.1 M KOH using a scan rate of 5 mV s^{-1} and an electrode rotation rate of 900 rpm. It is evident that the NPMC-900 catalyst does not show performance degradation during 700 potential cycling test, indicating that the NPMC is much more stable in alkaline solution than in acid medium.

Fig. 5 shows the Koutecky–Levich plots for the oxygen reduction reaction at 0.6 V in 0.5 M H_2SO_4 and 0.1 M KOH on the NPMC-900 before and after the potential cycling stability test. The dotted line is the theoretical data calculated for the four-electron reduction of oxygen. The slope of the plots allows us to check the consistency

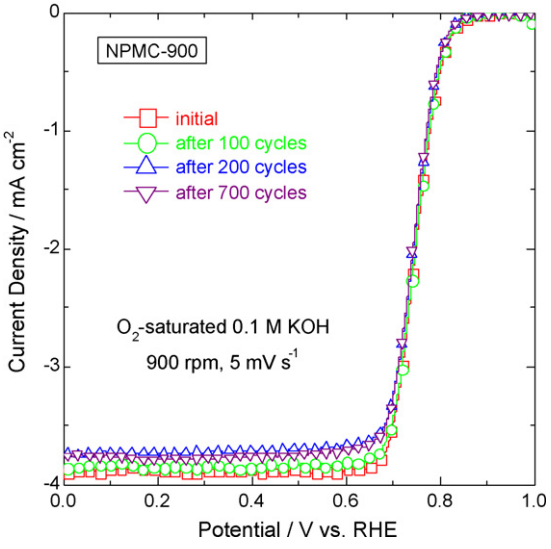

Fig. 4. Polarization curves for the oxygen reduction reaction in O_2-saturated 0.1 M KOH on non-precious metal catalysts heat-treated at 900 °C before and after the potential cycling stability test; scan rate: 5 mV s^{-1}; rotation rate: 900 rpm. The potential cycling was performed in N_2-saturated 0.1 M KOH with a scan rate of 10 mV s^{-1} between 0.8 and 1.2 V vs. RHE for 100, 200, and 700 cycles.

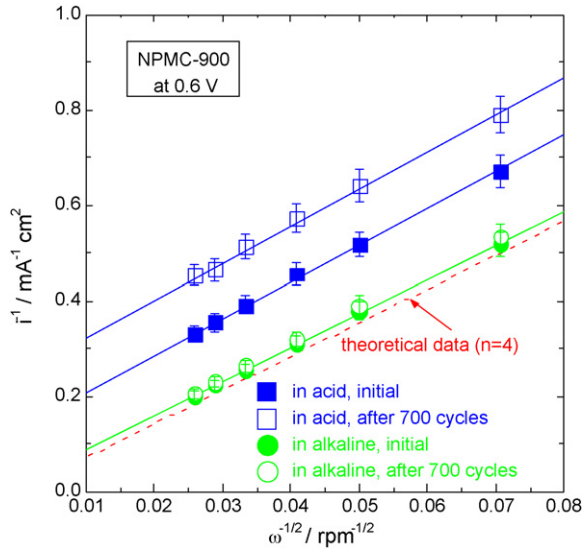

Fig. 5. Koutecky–Levich plots for the oxygen reduction reaction at 0.6 V vs. RHE in 0.5 M H_2SO_4 and 0.1 M KOH on non-precious metal catalysts heat-treated at 900 °C before and after the potential cycling stability test. The dotted line is the theoretical data calculated for the four-electron reduction of oxygen.

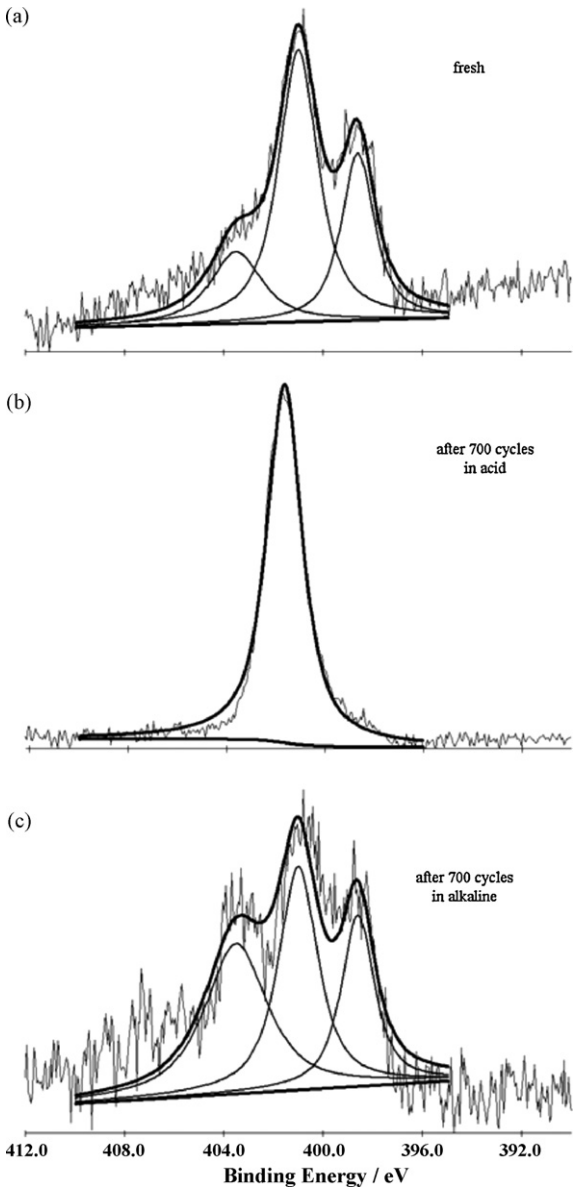

Fig. 6. XPS spectra of N 1s of (a) the fresh non-precious metal catalyst and the catalysts after the potential cycling stability test in (b) 0.5 M H_2SO_4 and (c) 0.1 M KOH for 700 cycles. The catalyst heat-treated at 900 °C was employed here.

with the theoretical values according to the equations:

$$\frac{1}{i} = \frac{1}{i_{kin}} + \frac{1}{i_l} \quad (3)$$

$$i_l = B\omega^{1/2} = 0.62nFD_0^{2/3}\nu^{-1/6}C_{O_2}\omega^{1/2} \quad (4)$$

where i is the measured current density, i_{kin} is the kinetic current density, i_l is the diffusion limited current density, B is the Levich slope, n is the number of electron exchanged in ORR, F is the Faraday constant, C_{O_2} is the bulk concentration of oxygen (1.3×10^{-6} mol cm^{-3}), D_{O_2} is the diffusion coefficient of oxygen in the bulk solution (1.7×10^{-5} cm^2 s^{-1}), ω is the rotation rate in rpm, and ν is the kinematic viscosity of the solution (0.01 cm^2 s^{-1}). As a result, the calculated n values for NPMC-900 in 0.5 M H_2SO_4 and 0.1 M KOH are 3.65 and 3.92, respectively, and are the same before and after the potential cycling stability test. This indicates that NPMC-900 in alkaline media catalyzes the ORR via a four-electron pathway to a greater extent than the catalyst in acid solution. The amount of H_2O_2 formed on NPMC-900 in alkaline environments is lower than in acid media.

Fig. 6 shows the XPS spectra of N 1s for the NPMC-900 before and after the potential cycling stability test in 0.5 M H_2SO_4 and 0.1 M KOH. According to the literature [29,30,44,45], the peaks of N 1s at 398.6 ± 0.3, 401.3 ± 0.3, and 403.3 ± 0.3 eV can be attributed to the pyridinic-N, graphitic-N, and pyridine-N-oxide, respectively. The pyridinic-N and graphitic-N are believed to play important roles in determining the activity of NPMCs [27–30,36–40]. As shown in Fig. 6, after the potential cycling stability test in alkaline electrolyte, the profile of the N 1s spectra of NPMC-900 is still similar to those of fresh catalyst. This may at least partially explain the high stability of NPMC for oxygen reduction under alkaline environments. In contrast, the N 1s spectra change from having three peaks to only one peak at 403.6 eV after the potential cycling test in acid electrolyte. According to the literature [29,30,44,45], the remaining peak at 403.6 eV may be assigned to both the graphitic-N and the protonated pyridinic-N formed in the acidic environment. This may be the reason for the rapid performance degradation of non-precious metal catalysts under acid conditions.

The high activity and stability of the NPMCs for the ORR in alkaline electrolyte make them promising catalyst candidates at the cathode of alkaline fuel cells (AFCs). The AFC was originally used on space missions to provide power and drinking water to the shuttle. Currently, AFCs are used predominantly in niche transportation applications such as powering forklift trucks, boats and submarines. To become competitive in mainstream commercial markets, AFCs have to become more cost effective [46]. Our future work will focus on the development of NPMC-based H_2–O_2 anion-exchange membrane fuel cells in collaboration with Tokuyama Corporation, Japan.

4. Conclusions

The electrocatalytic properties of non-precious metal catalysts (NPMCs) toward oxygen reduction under both acid and alkaline environments were studied by the rotating disk electrode (RDE) technique. The NPMCs were prepared through the pyrolysis of cobalt–iron–nitrogen chelate followed by the treatment combination of pyrolysis, acid leaching, and re-pyrolysis. A high activity of NPMCs for oxygen reduction in alkaline solution was demonstrated by a high onset potential of 0.92 V and a well-defined limiting current plateau. A potential cycling stability testing protocol was developed for the NPMCs. In acid solution, the performance degradation of NPMCs exhibits an exponential increase with increasing number of potential cycling, which is consistent with the long-term fuel cell stability test. In alkaline solution, the NPMC shows a much higher stability. The catalysts in alkaline media catalyze the ORR via four-electron pathway to a greater extent than that in acid solution. The XPS further demonstrated the excellent stability of the nitrogen-containing active sites in alkaline electrolyte when compared to the stability of the same catalyst in acid electrolyte. As suggested in our previous studies [28–30], the results presented in this work indicated that the observed decreased stability in the acid medium results from protonation of the pyridinic-N to pyridinic-N–H sites which are not active for oxygen reduction.

References

[1] R. Jasinski, Nature 201 (1964) 1212–1213.
[2] H. Jahnke, M. Schönbron, G. Zimmermann, Top. Curr. Chem. 61 (1976) 133–181.
[3] V.S. Bogatzky, M.R. Tarasevich, K.A. Radyushkina, O.E. Levina, S.I. Andrusyova, J. Power Sources 2 (1977) 233–240.
[4] S.L. Gupta, D. Tryk, I. Bae, W. Aldred, E.B. Yeager, J. Appl. Electrochem. 19 (1989) 19–27.
[5] M. Lefèvre, E. Proietti, F. Jaouen, J.-P. Dodelet, Science 324 (2009) 71–74.
[6] J.A.R. van Veen, H.A. Colijn, Ber. Bunsenges. Phys. Chem. 85 (1981) 700–704.
[7] G. Lalande, R. Côté, G. Tamizhmani, D. Guay, J.P. Dodelet, L. Dignard-Bailey, L.T. Weng, P. Bertrand, Electrochim. Acta 40 (1995) 2635–2646.

[8] G. Faubert, G. Lalande, R. Cote, D. Guay, J.P. Dodelet, L.T. Weng, P. Bertrand, G. Denes, Electrochim. Acta 41 (1996) 1689–1701.
[9] G. Lalande, R. Cote, D. Guay, J.P. Dodelet, L.T. Weng, P. Bertrand, Electrochim. Acta 42 (1997) 1379–1388.
[10] M. Lefevre, J.P. Dodelet, Electrochim. Acta 48 (2003) 2749–2760.
[11] E. Proietti, S. Ruggeri, J.P. Dodelet, J. Electrochem. Soc. 155 (2008) B340–B348.
[12] F. Charreteur, F. Jaouen, J.P. Dodelet, Electrochim. Acta 54 (2009) 6622–6630.
[13] A. Garsuch, K. MacIntyre, X. Michaud, D.A. Stevens, J.R. Dahn, J. Electrochem. Soc. 155 (2008) B953–B957.
[14] A. Garsuch, R. d'Eon, T. Dahn, O. Klepel, R.R. Garsuch, J.R. Dahn, J. Electrochem. Soc. 155 (2008) B236–B243.
[15] G. Wu, K. Artyushkova, M. Ferrandon, J. Kropf, D. Myers, P. Zelenay, ECS Trans. 25 (2009) 1299–1311.
[16] X. Li, C. Liu, W. Xing, T. Lu, J. Power Sources 193 (2009) 470–476.
[17] J. Maruyama, I. Abe, Chem. Mater. 17 (2005) 4660–4667.
[18] J. Maruyama, I. Abe, Chem. Mater. 18 (2006) 1303–1311.
[19] J. Maruyama, I. Abe, J. Electrochem. Soc. 154 (2007) B297–B304.
[20] J. Maruyama, J. Okamura, K. Miyazaki, Y. Uchimoto, I. Abe, J. Phys. Chem. C 112 (2008) 2784–2790.
[21] P. Gouerec, A. Biloul, O. Contamin, G. Scarbeck, M. Savy, J. Riga, L.T. Weng, P. Bertrand, J. Electroanal. Chem. 422 (1997) 61–75.
[22] P. Gouerec, M. Savy, J. Riga, Electrochim. Acta 43 (1998) 743–753.
[23] P. Gouerec, M. Savy, Electrochim. Acta 44 (1999) 2653–2661.
[24] H. Schulenburg, S. Stankov, V. Schu1nemann, J. Radnik, I. Dorbandt, S. Fiechter, P. Bogdanoff, H. Tributsch, J. Phys. Chem. B 107 (2003) 9034–9041.
[25] S. Kundu, T.C. Nagaiah, W. Xia, Y. Wang, S. Van Dommele, J.H. Bitter, M. Santa, G. Grundmeier, M. Bron, W. Schuhmann, M. Muhler, J. Phys. Chem. C 113 (2009) 14302–14310.
[26] V. Nallathambi, J.-W. Lee, S.P. Kumaraguru, G. Wu, B.N. Popov, J. Power Sources 183 (2008) 34–42.
[27] N. Subramanian, X. Li, V. Nallathambi, S. Kumaraguru, H. Colon-Mercado, G. Wu, J.-W. Lee, B.N. Popov, J. Power Sources 188 (2009) 38–44.
[28] B.N. Popov, X. Li, G. Liu, Int. J. Hydrogen Energy (2010), doi:10.1016/j.ijhydene, 2009.12.050.
[29] G. Liu, X. Li, P. Ganesan, B.N. Popov, Appl. Catal. B: Environ. 93 (2009) 156–165.
[30] G. Liu, X. Li, P. Ganesan, B.N. Popov, Electrochim. Acta 55 (2010) 2853–2858.
[31] N.P. Subramanian, S.P. Kumaraguru, H. Colon-Mercado, H. Kim, B.N. Popov, T. Black, D.A. Chen, J. Power Sources 157 (2006) 56–63.
[32] X. Li, S. Park, B.N. Popov, J. Power Sources 195 (2010) 445–452.
[33] X. Li, H.R. Colon-Mercado, G. Wu, J.-W. Lee, B.N. Popov, Electrochem. Solid State Lett. 10 (2007) B201–B205.
[34] M. Bron, S. Fiechter, P. Bogdanoff, H. Tributsch, Fuel Cells 2 (2003) 137–142.
[35] S. Baranton, C. Coutanceau, C. Roux, F. Hahn, J.-M. Leger, J. Electroanal. Chem. 577 (2005) 223–234.
[36] E. Yeager, Electrochim. Acta 29 (1984) 1527–1537.
[37] K. Wiesener, Electrochim. Acta 31 (1986) 1073–1078.
[38] P.H. Matter, L. Zhang, U.S. Ozkan, J. Catal. 239 (2006) 83–96.
[39] S. Maldonado, K.J. Stevenson, J. Phys. Chem. B 109 (2005) 4707–4716.
[40] K.A. Kurak, A.B. Anderson, J. Phys. Chem. C 113 (2009) 6730–6734.
[41] DOE cell component accelerated stress test protocols for PEM fuel cells, http://www1.eere.energy.gov/hydrogenandfuelcells/fuelcells/pdfs/component_durability_profile.pdf.
[42] H.-S. Choo, T. Kinumoto, M. Nose, K. Miyazaki, T. Abe, Z. Ogumi, J. Power Sources 185 (2008) 740–746.
[43] S.Lj. Gojkovic, S. Gupta, R.F. Savinell, J. Electroanal. Chem. 462 (1999) 63–72.
[44] J.R. Pels, F. Kapteijn, J.A. Moulijn, Q. Zhu, K.M. Thomas, Carbon 33 (1995) 1641–1653.
[45] F. Jaouen, J. Herranz, M. Lefevre, J.P. Dodelet, U.I. Kramm, I. Herrmann, P. Bogdanoff, J. Maruyama, T. Nagaoka, A. Garsuch, J.R. Dahn, T. Olson, S. Pylypenko, P. Atanassov, E.A. Ustinov, ACS Appl. Mater. Interfaces 1 (2009) 1623–1639.
[46] G. Crawley, Fuel Cell Today March, 2006, pp. 1–10.